IOPscience iopscience.iop.org

Home Search Collections Journals About Contact us My IOPscience

Applying computational nanomaterials design to the reactive ion etching of NiO thin films—a preliminary investigation

This article has been downloaded from IOPscience. Please scroll down to see the full text article.

2007 J. Phys.: Condens. Matter 19 365210

(http://iopscience.iop.org/0953-8984/19/36/365210)

View the table of contents for this issue, or go to the journal homepage for more

Download details:
IP Address: 129.252.86.83
The article was downloaded on 29/05/2010 at 04:37

Please note that terms and conditions apply.

IOP PUBLISHING JOURNAL OF PHYSICS: CONDENSED MATTER

J. Phys.: Condens. Matter **19** (2007) 365210 (7pp) doi:10.1088/0953-8984/19/36/365210

Applying computational nanomaterials design to the reactive ion etching of NiO thin films—a preliminary investigation

M David[1], R Muhida[1], T Roman[1], S Kunikata[1], W A Diño[2], H Nakanishi[1], H Kasai[1], F Takano[3], H Shima[3] and H Akinaga[3]

[1] Graduate School of Engineering, Osaka University, Suita 565-0871, Japan
[2] Center for Promotion of Research in Nanoscience and Nanotechnology, Osaka University, Toyonaka 560-8531, Japan
[3] National Institute of Advanced Industrial Science and Technology (AIST), Japan

Received 19 December 2006, in final form 24 May 2007
Published 24 August 2007
Online at stacks.iop.org/JPhysCM/19/365210

Abstract

We have developed and proposed a model for reactive ion etching (RIE) process design of nickel oxide thin films using a computational materials design based on *ab initio* calculations. On etching NiO, we found that it was necessary to have hydrogen-based reactive gases in the initial state in order to enhance RIE (e.g. NH_3, CH_4). We strongly suggest the use of CH_4 or any H-based gas source other than CHF_3 to enhance RIE process.

1. Introduction

The surface of metal oxides, specifically transition metal oxides, has been extensively studied in recent years because the development of nanoscale processing techniques has enabled us to fabricate nanostructures. In particular, nickel oxide shows bistable conductivity switching properties and can have potential applications for nonvolatile memory devices such as resistance random access memory (RRAM) [1–3]. Recently, the reactive ion etching (RIE) process has been widely used for ultrafine-fabrication in the electronics industry. However, it is hard to determine the optimum RIE conditions like vacuum pressure, gas composition and plasma activity for the etching of magnetic materials. Several experiments have demonstrated RIE processes of transition metal (TM) compounds such as Ni–Fe, Ni–Fe–Co and Co–Fe, employing two basic plasma chemistries of Cl_2 and CO/NH_3 [4–6] in these investigations. The CO/NH_3 is said to promote the formation of volatile metal carbonyls such as $Ni(CO)_4$ and $Fe(CO)_5$. For RIE of surface oxides, CHF_3 is suggested to be compatible with SiO_2 [7]. Experimentalists from AIST and ULVAC used a $CHF_3/N_2/O_2$ gas combination to etch NiO, CoO and CuO and were successful in carrying out RIE with a minimum amount of N_2. The experimental details of this study will be reported in another paper.

 © 2007 IOP Publishing Ltd Printed in the UK

With the recent developments in computational techniques, coupled with rapid progress in computer efficiency, *ab initio*/first-principles-based *Computational Materials Design* (CMD®) is now a reality [8, 9]. Its impact and influence on industrial research and development should increase in the coming years. One of its applications is to design and develop effective and efficient methods for fabricating electronic and magnetic devices. With the development of CMD, we design a model for the RIE process based on *ab initio* calculations. We perform density functional theory (DFT)-based calculations of the total energy and electronic structure of the surface and molecules. Working hand-in-hand with the experimental group, we test the ideas laid out in our design and compare them with the experimental results. We have established the computational process design for NiFe and CoFe alloy thin films for RIE [10–15] and the results, most especially for NiFe, are in good agreement with experimental results [10].

In this paper, we propose a model for the etching process of NiO thin films. This investigation is an attempt to predict beforehand the gas combinations necessary for successfully etching a metal oxide surface to be used to fabricate nanomagnetic materials. We evaluate the reactivity on the basis of the change in total energy. There are many possible gas combinations to produce different products, but we considered those by-products that are volatile. Moreover, the RIE process involves complex interactions of ions of gas molecules and surfaces. Basically, this can be regarded as an initial investigation since it only considers the total energy of the different states. Furthermore, the intermediate states only include interaction of gas molecules *on* the surfaces at a time and do not involve interactions between gas molecules near the surface. However, this can be considered a groundwork in the understanding of the reactivity in etching the NiO surface and a means of decreasing the RIE processing period for NiO thin films in terms of determining the gas combinations and the probable by-products. In addition to this, the outcome of this study may be applied not only for ion-based etching but also for neutral-based etching processes.

2. Model and method

In the computational process design, we consider three specific states of the RIE process: the initial, intermediate and final states, similar to those used in the RIE of NiFe [10]. In the initial state, a gas molecule is far from the metal surface. The molecule does not interact with the surface. In the intermediate state, the molecule is close to the surface, around 1.8–3 Å, and the position of the molecule on the surface has to be considered. In the final state, one atom is taken from the surface and the etched compounds and the by-products are in a vacuum leaving a vacancy on the surface. In this study, we considered the formation of a Ni vacancy on the NiO surface.

As for the initial investigation, the supercell is composed of a one-layer slab of NiO(100) (2×2) with 8.32 Å as the cell length and width and a vacuum distance of 12 Å. We considered the antiferromagnetic state of NiO. We performed computations on the generalized gradient approximation (GGA) of the DFT using a plane wave basis set. We used 16 k-points and adopted a 60 Ryd energy cutoff for kinetic energy.

In terms of choosing the gas combinations, we consider the gas combinations used in the experiments and find the combinations of by-products that will give lower energies for the final state. In addition, the by-products should be volatile, stable and be stoichiometrically possible for the conservation of the reaction process. The main by-product for NiO according to previous studies is $Ni(CO)_4$ [4–6, 10].

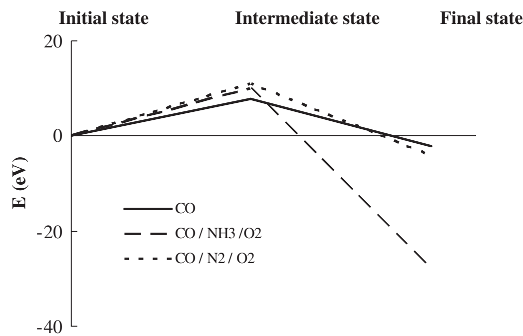

Figure 1. Reaction paths for CO–gas combinations.

3. Results and discussion

The details of the etching characteristics for the NiO are described in this section. First, we used CO gas as the main reactive gas and then later combined it with other gases. The etching process with this gas is represented by the following chemical reactions:

3.1. CO–gas combinations

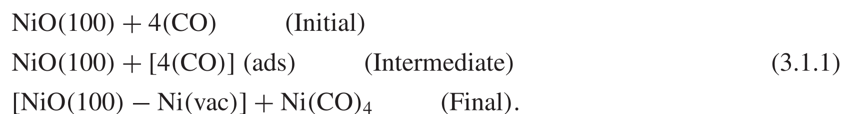

$$\begin{aligned} &\mathrm{NiO(100)} + 4(\mathrm{CO}) \qquad \text{(Initial)} \\ &\mathrm{NiO(100)} + [4(\mathrm{CO})]\ (\mathrm{ads}) \qquad \text{(Intermediate)} \\ &[\mathrm{NiO(100)} - \mathrm{Ni(vac)}] + \mathrm{Ni(CO)_4} \qquad \text{(Final)}. \end{aligned} \tag{3.1.1}$$

Here (ads) means that the distance between a molecule and the NiO surface ranges from approximately 1.8 to 3.0 Å and (hollow) means that there is a Ni vacancy in the surface of the unit cell. The following are the chemical reactions for different gas combinations with CO based on the $CO/NH_3/O_2$ combinations for NiFe [6] and the possibility of combining CO and N_2:

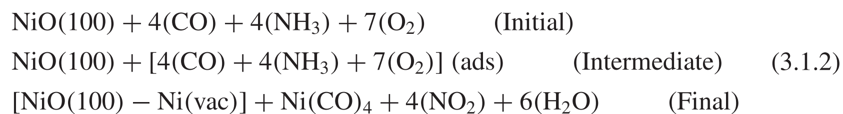

$$\begin{aligned} &\mathrm{NiO(100)} + 4(\mathrm{CO}) + 4(\mathrm{NH_3}) + 7(\mathrm{O_2}) \qquad \text{(Initial)} \\ &\mathrm{NiO(100)} + [4(\mathrm{CO}) + 4(\mathrm{NH_3}) + 7(\mathrm{O_2})]\ (\mathrm{ads}) \qquad \text{(Intermediate)} \\ &[\mathrm{NiO(100)} - \mathrm{Ni(vac)}] + \mathrm{Ni(CO)_4} + 4(\mathrm{NO_2}) + 6(\mathrm{H_2O}) \qquad \text{(Final)} \end{aligned} \tag{3.1.2}$$

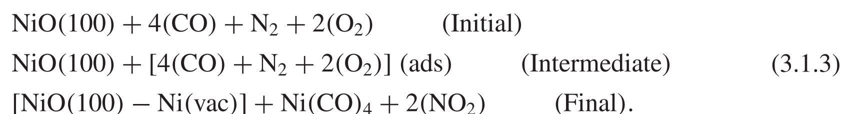

$$\begin{aligned} &\mathrm{NiO(100)} + 4(\mathrm{CO}) + \mathrm{N_2} + 2(\mathrm{O_2}) \qquad \text{(Initial)} \\ &\mathrm{NiO(100)} + [4(\mathrm{CO}) + \mathrm{N_2} + 2(\mathrm{O_2})]\ (\mathrm{ads}) \qquad \text{(Intermediate)} \\ &[\mathrm{NiO(100)} - \mathrm{Ni(vac)}] + \mathrm{Ni(CO)_4} + 2(\mathrm{NO_2}) \qquad \text{(Final)}. \end{aligned} \tag{3.1.3}$$

The energy differences for the different states with respect to the initial energy and the reaction pathways of NiO thin film for these combinations of reactive gases are presented in figure 1. We can observe that the final state is more stable than the intermediate state. The gas combination that gives the lowest energy in the final state is the $CO/NH_3/O_2$ combination, then the $CO/N_2/O_2$ and lastly CO alone, as shown in figure 1.

Figure 2 shows the reaction path for NH_3 combinations with the following chemical reactions:

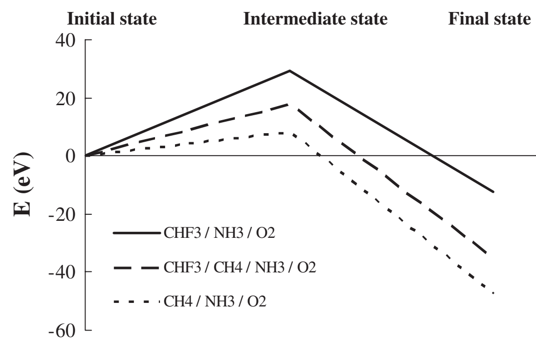

Figure 2. Reaction paths for NH_3–gas combinations.

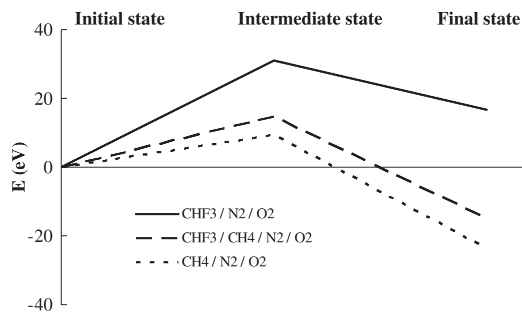

Figure 3. Reaction paths for N_2–gas combinations.

3.2. NH_3–gas combinations

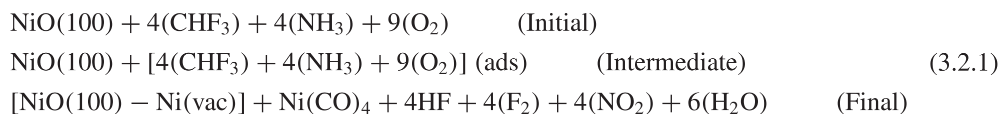

$$\begin{aligned}&\mathrm{NiO(100) + 4(CHF_3) + 4(NH_3) + 9(O_2)} \quad \text{(Initial)}\\&\mathrm{NiO(100) + [4(CHF_3) + 4(NH_3) + 9(O_2)]\ (ads)} \quad \text{(Intermediate)}\\&\mathrm{[NiO(100) - Ni(vac)] + Ni(CO)_4 + 4HF + 4(F_2) + 4(NO_2) + 6(H_2O)} \quad \text{(Final)}\end{aligned} \tag{3.2.1}$$

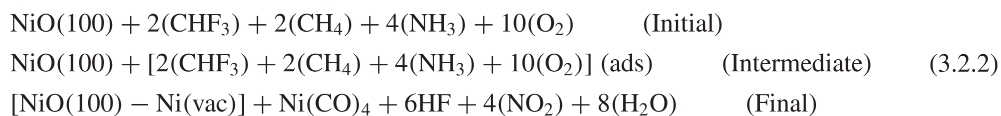

$$\begin{aligned}&\mathrm{NiO(100) + 2(CHF_3) + 2(CH_4) + 4(NH_3) + 10(O_2)} \quad \text{(Initial)}\\&\mathrm{NiO(100) + [2(CHF_3) + 2(CH_4) + 4(NH_3) + 10(O_2)]\ (ads)} \quad \text{(Intermediate)}\\&\mathrm{[NiO(100) - Ni(vac)] + Ni(CO)_4 + 6HF + 4(NO_2) + 8(H_2O)} \quad \text{(Final)}\end{aligned} \tag{3.2.2}$$

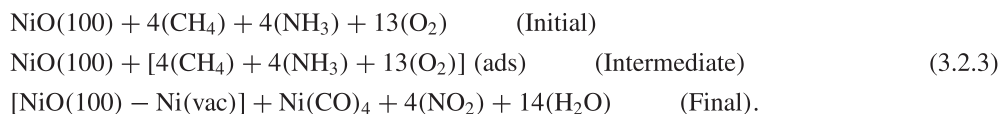

$$\begin{aligned}&\mathrm{NiO(100) + 4(CH_4) + 4(NH_3) + 13(O_2)} \quad \text{(Initial)}\\&\mathrm{NiO(100) + [4(CH_4) + 4(NH_3) + 13(O_2)]\ (ads)} \quad \text{(Intermediate)}\\&\mathrm{[NiO(100) - Ni(vac)] + Ni(CO)_4 + 4(NO_2) + 14(H_2O)} \quad \text{(Final).}\end{aligned} \tag{3.2.3}$$

From the two figures, we can see that $CH_4/NH_3/O_2$ has the lowest energy in the final state (3.2.3). It can be noted that the by-products that give the lowest energy are H_2O and NO_2. The $CHF_3/NH_3/O_2$ combination with F_2 as one of the by-products (3.2.1) has a higher energy than the $CHF_3/CH_4/NH_3/O_2$ combination without including F_2 in the by-products (3.2.2). If NH_3 is replaced by N_2, the reaction paths will be as shown in figure 3 with the following chemical reactions:

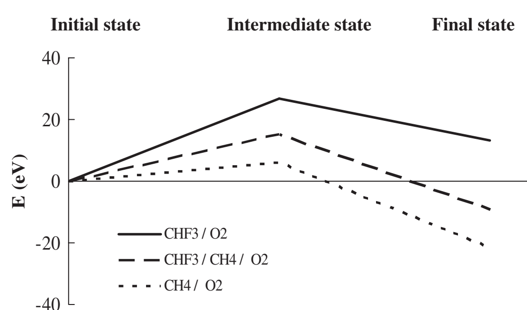

Figure 4. Reaction paths for gas combinations without N_2.

3.3. N_2–gas combinations

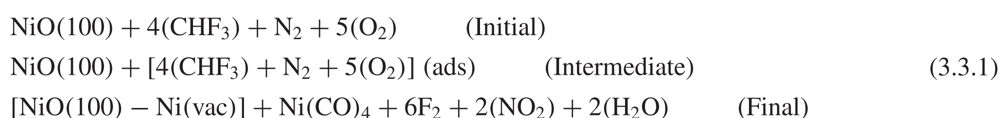

$$\begin{aligned} &\mathrm{NiO(100) + 4(CHF_3) + N_2 + 5(O_2)} \quad \text{(Initial)}\\ &\mathrm{NiO(100) + [4(CHF_3) + N_2 + 5(O_2)]\ (ads)} \quad \text{(Intermediate)}\\ &\mathrm{[NiO(100) - Ni(vac)] + Ni(CO)_4 + 6F_2 + 2(NO_2) + 2(H_2O)} \quad \text{(Final)} \end{aligned} \qquad (3.3.1)$$

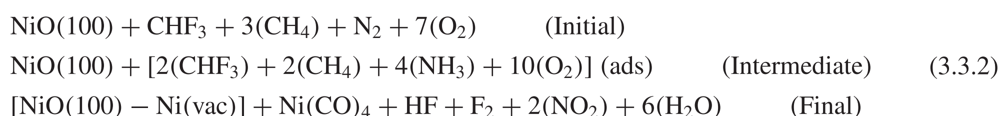

$$\begin{aligned} &\mathrm{NiO(100) + CHF_3 + 3(CH_4) + N_2 + 7(O_2)} \quad \text{(Initial)}\\ &\mathrm{NiO(100) + [2(CHF_3) + 2(CH_4) + 4(NH_3) + 10(O_2)]\ (ads)} \quad \text{(Intermediate)}\\ &\mathrm{[NiO(100) - Ni(vac)] + Ni(CO)_4 + HF + F_2 + 2(NO_2) + 6(H_2O)} \quad \text{(Final)} \end{aligned} \qquad (3.3.2)$$

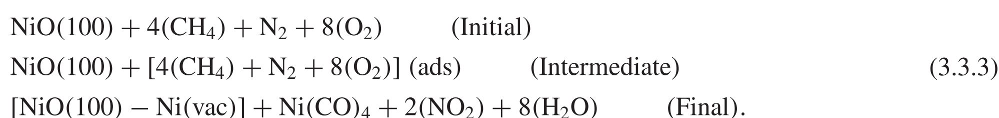

$$\begin{aligned} &\mathrm{NiO(100) + 4(CH_4) + N_2 + 8(O_2)} \quad \text{(Initial)}\\ &\mathrm{NiO(100) + [4(CH_4) + N_2 + 8(O_2)]\ (ads)} \quad \text{(Intermediate)}\\ &\mathrm{[NiO(100) - Ni(vac)] + Ni(CO)_4 + 2(NO_2) + 8(H_2O)} \quad \text{(Final).} \end{aligned} \qquad (3.3.3)$$

Again, we can observe in figure 3 that the combination that gives the lowest energy is the $CH_4/N_2/O_2$ combination with by-products NO_2 and H_2O (3.3.3), followed by $CHF_3/CH_4/N_2/O_2$ (3.3.2) then $CHF_3/N_2/O_2$ has the highest energy (3.3.1). From this we can say that the hydrogen in the gas source makes the reactivity more favourable (i.e. CH_4) and, unlike in SiO_2, halogens such as F may produce poor reactivity for NiO. We also considered the elimination of N gas in the following combinations with the reaction paths given in figure 4:

3.4. Without N_2–gas combinations

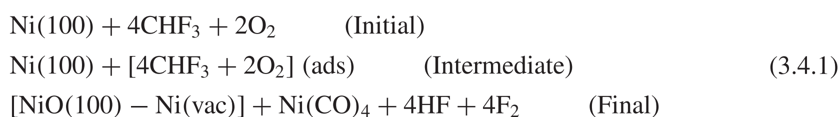

$$\begin{aligned} &\mathrm{Ni(100) + 4CHF_3 + 2O_2} \quad \text{(Initial)}\\ &\mathrm{Ni(100) + [4CHF_3 + 2O_2]\ (ads)} \quad \text{(Intermediate)}\\ &\mathrm{[NiO(100) - Ni(vac)] + Ni(CO)_4 + 4HF + 4F_2} \quad \text{(Final)} \end{aligned} \qquad (3.4.1)$$

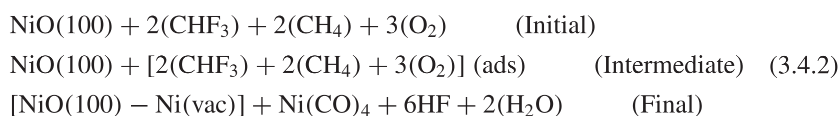

$$\begin{aligned} &\mathrm{NiO(100) + 2(CHF_3) + 2(CH_4) + 3(O_2)} \quad \text{(Initial)}\\ &\mathrm{NiO(100) + [2(CHF_3) + 2(CH_4) + 3(O_2)]\ (ads)} \quad \text{(Intermediate)}\\ &\mathrm{[NiO(100) - Ni(vac)] + Ni(CO)_4 + 6HF + 2(H_2O)} \quad \text{(Final)} \end{aligned} \qquad (3.4.2)$$

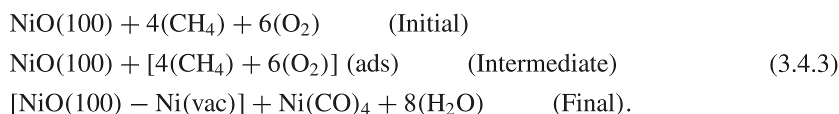

$$\begin{aligned} &\mathrm{NiO(100) + 4(CH_4) + 6(O_2)} \quad \text{(Initial)}\\ &\mathrm{NiO(100) + [4(CH_4) + 6(O_2)]\ (ads)} \quad \text{(Intermediate)}\\ &\mathrm{[NiO(100) - Ni(vac)] + Ni(CO)_4 + 8(H_2O)} \quad \text{(Final).} \end{aligned} \qquad (3.4.3)$$

As expected, the CH_4/O_2 gas source combination yields the lowest total energy, followed by the $CHF_3/CH_4/O_2$ combination, and the CHF_3/O_2 combination yields the highest energy. It can also be noted that the CHF_3/O_2 gas source yields a lower energy than with $CHF_3/N_2/O_2$. This means that minimal N_2, or no N_2 at all, gives better reactivity. On the other hand, $CHF_3/CH_4/N_2/O_2$ and $CH_4/N_2/O_2$ instigate better reactivity than without N_2. The reactivity may be attributed more to the hydrogen content of the source gas than to the presence of N_2, as can be seen in the energy differences from figures 2 and 3.

There are many possibilities for the reaction paths for etching metal oxide surfaces and we are just beginning to scrutinize the complexities of the RIE process. We are continuing this study to investigate the effect of difference gas combinations in increasing the efficiency of the RIE process and extending the number of layers in order to emulate the behaviour of the NiO thin film.

4. Conclusion

We were able to develop and propose a model for the RIE process design of nickel oxide thin films using computational materials design based on *ab initio* calculations. On etching NiO, we found that it was necessary to have hydrogen-based reactive gases in the initial state in order to enhance RIE (e.g. NH_3, CH_4). We strongly suggest the use of CH_4 or any H-based gas source other than CHF_3 to enhance the RIE process. Experimental verification and modification of our model is under way. This model can be used not only for ion-based etching but also for neutral-based etching processes.

Acknowledgments

This work is partly supported by NEDO and the Ministry of Education, Culture, Sports, Science and Technology of Japan (MEXT) through Grants-in-Aid for Scientific Research on Priority Areas (Developing Next Generation Quantum Simulators and Quantum-Based Design Techniques), and through Grants-in-Aid for the 21st Century Center of Excellence (COE) Program 'Core Research and Advance Education Center for Material Science and Nano-Engineering' supported by the Japan Society for the Promotion of Science (JSPS). One of the authors (MD) acknowledges supports from the Marubun Research Promotion Foundation. Calculations were performed using the computer facilities of the Institute for Solid State Physics (ISSP) Supercomputer Center (University of Tokyo) and the Japan Atomic Energy Research Institute (ITBL, JAERI).

References

[1] Seo S, Lee M J, Seo D H, Jeoung E J, Suh D S, Joung Y S, Yoo I K, Hwang I R, Kim S H, Byun I S, Kim J S, Choi J S and Park B H 2004 *Appl. Phys. Lett.* **85** 263507
[2] Zhuang W W, Pan W, Ulrich B D, Lee J J, Stecker L, Burmaster A, Evans D R, Hsu S T, Tajiri M, Shimaoka A, Inoue K, Naka T, Awaya N, Sakiyama K, Wang Y, Liu S Q, Woo N J and Ignatiev A 2002 *Proc. Tech. Dig. Int. Electron Devices Mtg (San Francisco)* p 193
[3] Chen A, Haddad S, Woo Y C, Fang T N, Lan Z, Avanzino S, Pangrle S, Buynoski M, Rathor M, Cai W, Tripsas N, Bill C and Taguchi M 2005 *Proc. Tech. Dig. Int. Electron Devices Mtg (Washington, DC)* p 765
[4] Mukai T, Hada H, Tahara S, Yoda H and Samukawa S 2006 *Japan. J. Appl. Phys.* **45** 5542–4
[5] Cho H, Lee K P, Hahn Y B, Lambers E S and Pearton S J 2000 *J. Vac. Sci. Technol.* A **18** 1273–7
[6] Nakatani I 1996 *IEEE Trans. Magn.* **32** 4448–51
[7] Chae H, Vitale S A and Sawin H 2003 *J. Vac. Sci. Technol.* A **21** 381–7

[8] Kasai H *et al* (ed) 2005 *Introduction to Computational Material Design—From the Basics to Actual Applications* (Osaka: Osaka University)
[9] Nanospintronics design and realization http://www.dyn.ap.eng.osaka-u.ac.jp/NDR
[10] Watanabe S, Diño W A, Nakanishi H, Kasai H and Akinaga H 2005 *Japan. J. Appl. Phys.* **44** 893–4
[11] Matsumoto S and Kasai H 2006 *Advanced Industrial Science and Technology (AIST) Workshop on Functional Oxides—Correlated Electrons for Non-Volatile Memory Applications*
[12] Kanazawa T, Motoyama S, Wakayama T and Akinaga H 2006 *Proc. 6th Int. Conf. on Reactive Plasmas/Symp. on Plasma Processing (ICRP/SPP)-23* p 471
[13] Matsumoto S, Diño W A, David M, Muhida R, Nakanishi H, Akinaga H and Kasai H 2006 *Proc. 6th Int. Conf. on Reactive Plasmas/Symp. on Plasma Processing (ICRP/SPP)-23* p 481
[14] Akinaga H, Takano F, Matsumoto S and Diño W A 2005 *J. Vac. Soc. Japan* **49** 716–21
[15] Matsumoto S, Diño W A, David M, Muhida R, Roman T, Kunikata S, Takano F, Akinaga H and Kasai H 2007 *J. Vac. Soc. Japan* **50** 437–9